



# Thermo-elasto-plastic modeling of saturated clays under undrained conditions

Wei Cheng, Peng-Yun Hong, Jean-Michel Pereira, Yu-Jun Cui, Anh Minh A.M. Tang, Ren-Peng Chen

## ► To cite this version:

Wei Cheng, Peng-Yun Hong, Jean-Michel Pereira, Yu-Jun Cui, Anh Minh A.M. Tang, et al.. Thermo-elasto-plastic modeling of saturated clays under undrained conditions. *Computers and Geotechnics*, 2020, 125, 31 p. 10.1016/j.compgeo.2020.103688 . hal-02880511

**HAL Id: hal-02880511**

**<https://enpc.hal.science/hal-02880511>**

Submitted on 25 Jun 2020

**HAL** is a multi-disciplinary open access archive for the deposit and dissemination of scientific research documents, whether they are published or not. The documents may come from teaching and research institutions in France or abroad, or from public or private research centers.

L'archive ouverte pluridisciplinaire **HAL**, est destinée au dépôt et à la diffusion de documents scientifiques de niveau recherche, publiés ou non, émanant des établissements d'enseignement et de recherche français ou étrangers, des laboratoires publics ou privés.

# Thermo-elasto-plastic modeling of saturated clays under undrained conditions

Wei Cheng<sup>a</sup>, Peng-yun Hong<sup>b</sup>, Jean-Michel Pereira<sup>b,\*</sup>, Yu-jun Cui<sup>b</sup>,

Anh Minh Tang<sup>b</sup>, Ren-peng Chen<sup>a</sup>

<sup>a</sup>*Zhejiang University, Institute of Geotechnical Engineering, 310058, Hangzhou, China*

<sup>b</sup>*Navier, Ecole des Ponts, Univ Gustave Eiffel, CNRS, Marne-la-Vallée, France*

## Abstract:

This paper aims to model the thermo-mechanical behavior of saturated clays under undrained conditions. Classic thermo-hydro-mechanical formulations obtained using different approaches were compared and discussed, showing their compatibility and differences. A thermo-elasto-plastic model called TEAM, using a two-surface approach, was developed for saturated clays under undrained conditions in the framework of thermo-poro-mechanics. The aim of the model is to predict a smooth transition between the elastic and elastoplastic states. Two additional physical parameters, namely volumetric thermal expansion coefficient and pore water compressibility, were back analyzed from the results of the undrained heating tests. By simulating experiments found in the literature, it was shown that this model is appropriate in capturing the evolution of pore water pressure of saturated clays under non-isothermal undrained conditions.

*Keywords:* clays; elasto-plastic model; temperature effects; undrained clay behavior; thermal failure; validation

## 1. Introduction

The thermo-mechanical behavior of clays has been widely investigated over the past decades through the analysis of geomechanical problems such as nuclear waste geological disposals and reservoir engineering. It is worth noting that under undrained heating conditions excess pore water pressure in saturated clays is induced because of the thermal expansion of water which is higher than that of the soil skeleton. For instance, considering a temperature range between 20 °C and 90 °C in geoenvironmental applications, the volumetric thermal expansion coefficient of pore water is around 6 to 18 times that of the soil skeleton for clays (e.g. Boom clay, Callovo-Oxfordian claystone, Opalinus claystone) [1, 2, 3, 4, 5]. This effect will lead to a decrease in mean effective stress, which might lead to a critical situation in engineering practice. It is therefore important to investigate the thermo-mechanical behavior of clays under undrained condition.

Various thermo-mechanical constitutive models for saturated clays were developed in the context of elastoplasticity and critical state theory (e.g. [6, 7, 8, 9, 10, 11]). These elastoplastic constitutive models are formulated in terms of effective stress and temperature based on drained heating tests, allowing the description of the thermo-mechanical behavior of the soil skeleton. The evaluation of the pore water pressure and the undrained behavior can be predicted by imposing an extra condition such as a volumetric condition even though the effective stress path is not given during loading. It should be pointed out that the undrained behavior prediction was not considered in some existing constitutive models (e.g. [8, 9]). In some others (e.g. [6, 7, 10, 11]), different extra conditions were applied for undrained behavior analysis. Hueckel *et al.* [6, 12] analyzed the undrained heating process by combining the thermal volume change of pore water and the thermo-mechanical model for skeleton thermo-elasto-plasticity developed from the well-known Cam-Clay model. Robinet *et al.* [7] and also Yao *et al.* [11] predicted the undrained behavior by imposing a constant volume condition as classically done in the isothermal undrained condition. However, the volume change of the clays in the undrained thermal mechanical loading conditions cannot be neglected and does not hold constant due to the thermal expansion of the clay mass [13]. This expansion has a crucial importance in undrained heating analysis as shown by some researchers ([14, 15]). Formally, undrained condition for both isothermal and non-isothermal evolutions should refer to evolutions under constant mass of water condition. Graham *et al.* [16] calculated the thermal volumetric strain for undrained heating analysis by simply assuming a constant undrained volumetric thermal

coefficient based on experimental results. Laloui and François [10] addressed the behavior under undrained non-isothermal condition within the framework of thermo-mechanics of saturated porous media as developed by Lewis and Schrefler [17].

The co-existence of different volumetric conditions to model the thermomechanical behavior of saturated clays under undrained condition suggests the necessity to clarify and provide a rigorous approach to this problem. Although efforts have been made to develop thermo-hydro-mechanical formulations for saturated clays (or porous media) by a number of researchers (e.g. [18, 19]), progress is still required in the framework of thermo-elasto-plasticity of the soil skeleton. In addition, the volumetric thermal expansion coefficient of pore water in low-porosity clay is found to be different from that of bulk water by Baldi *et al.* [20]. This peculiar phenomenon is supported by other experimental observations [21, 22]. This feature should be taken into account in the determination of volumetric thermal expansion coefficient of pore water in saturated clays for the pore water pressure calculation.

Besides this important issue related to the governing condition for the undrained test, the thermo-mechanical model for the soil skeleton would greatly influence the undrained behavior prediction. Hong *et al.* [23] have developed a two-surface thermo-mechanical model called TEAM in the context of elasto-plasticity theory, with emphasis put on describing some important features of the thermo-mechanical behavior of natural clay evidenced experimentally such as the limited thermo-mechanical elastic zone and the smooth transition from the elastic behavior to the plastic one. However, it should be pointed out that the formulation of TEAM model is restricted to and validated for drained conditions. In this study, the thermo-elasto-plastic model TEAM is extended to account for undrained conditions, in the sense of constant mass of pore water.

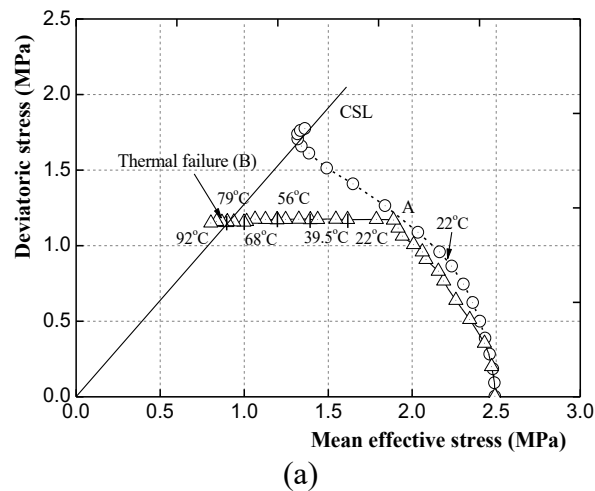
The main features of temperature effects on undrained saturated clays are first briefly analyzed. Then, the thermo-hydro-mechanical equations proposed by Campanella and Mitchell [14], Lewis and Schrefler [17] and Coussy [18] are recalled, compared and discussed, showing the compatibility and difference among them. Afterwards, the thermo-hydro-mechanical elasto-plastic constitutive formulation under undrained condition for saturated clays is presented in the framework of TEAM model. The procedure for parameter determination is then described. Finally, the TEAM model under undrained conditions is validated by simulating experiments on natural Boom Clay and reconstituted Pontida Clay.

Throughout this paper, the sign convention of soil mechanics is used, that is contractive strain and compressive (effective and total) stress are taken as positive.

## 2. Temperature effects under undrained conditions

Experimental evidences (e.g. [13]) clearly show that excess pore water pressure is induced during undrained heating of saturated clays. The mechanism of excess pore water pressure development upon heating can be simply analyzed. Saturated clays are composed of mineral solid (solid grains) and pore water. The soil skeleton can be defined as the part formed by the mineral solid and the pore space full of pore water. Due to heating, the temperature of soil skeleton and pore water will increase so that they will experience volumetric expansion. Since pore water expands more than the soil skeleton, its pressure tends to increase. If the heating process is performed under drained conditions (provided that the characteristic time of pressure diffusion is much shorter than the characteristic time of heating), pore water will be able to drain out of the specimen with no significant thermally induced excess pore water pressure. However, under undrained or partially drained conditions, since pore water cannot be expelled fast enough, excess pore water pressure will build up.

Especially under high deviatoric stress conditions, the pressurization of pore water induced by heating would bring the effective stress path close to the critical state line. A possible “thermal failure” could occur under these circumstances. Such thermally induced failure was observed by Hueckel et al. [12] in a laboratory experiment on reconstituted Pontida Clay as plotted in Fig.1, in which failure occurred when temperature was increased from 22 °C to 92 °C (path from A to B) under undrained condition and constant (total) stresses. At critical state, no further excess pore pressure develops.



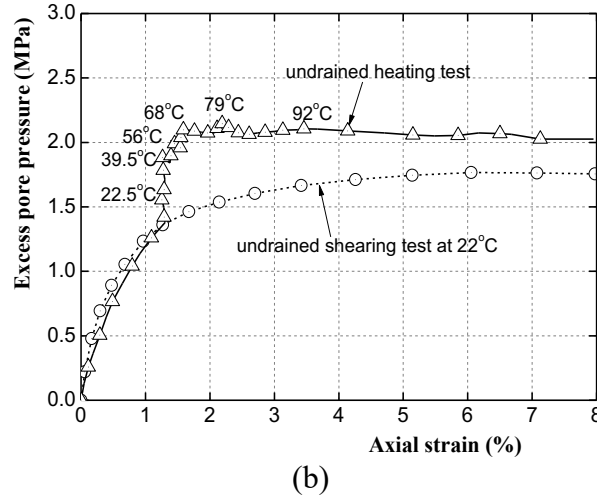


**Fig.1** Undrained heating test of reconstituted Pontida clay: (a) effective stress path; (b) excess pore pressure versus axial strain

### 3. Thermo-hydro-mechanical background

Campanella and Mitchell [14] initiatively gave the expression for pore water pressure variation along thermal mechanical loading paths under undrained condition using a simple governing equation for the volume change of total clay mass. Lewis and Schrefler [17] combined the mass balance equation with Darcy's law for the liquid phase in the pore space of porous media under non-isothermal condition. Coussy [18] analyzed this process and derived the equations in a thermo-poro-mechanical framework. In this section, these works are investigated in terms of compatibility in undrained heating analysis and compared to each other. To make the comparison easier, all the work is considered in the thermo-elastic zone. Note that the mineral solid is considered as compressible in all the cases.

#### 3.1. Expressions after Campanella and Mitchell (1968)

Under undrained condition, the volume change of the total soil mass due to both temperature and stress changes is equal to the sum of volume changes of mineral solid and pore water. The expression can be written as:

$$(dV_s)_{dT} + (dV_s)_{dp} + (dV_w)_{dT} + (dV_w)_{dp} = (dV)_{dT} + (dV)_{dp} \quad (1)$$

where  $dV_s$ ,  $dV_w$  and  $dV$  are volume changes of mineral solid, pore water and clay mass, respectively, and the subscripts  $dT$  and  $dp$  denote 'due to' temperature change and mean total stress change, respectively.

The volume change of the mineral solid due to temperature change and total stress change can be respectively expressed as:

$$(dV_s)_{dT} = V_s \alpha_s dT \quad (2)$$

and

$$(dV_s)_{dp} = -V_s C_s du - V_s C_s dp' \quad (3)$$

where  $\alpha_s$  and  $C_s$  are the volumetric thermal expansion coefficient and the volumetric compressibility of mineral solid, respectively,  $V_s$  is the current volume of mineral solid,  $du$  is the pore water pressure change,  $dp'$  is the mean effective stress change defined as  $dp' = dp - du$  with  $dp$  being the total mean stress change.

The volume change of pore water due to temperature change and water pressure change can be respectively expressed as:

$$(dV_w)_{dT} = V_w \alpha_w dT \quad (4)$$

and

$$(dV_w)_{dp} = -V_w C_w du \quad (5)$$

where  $\alpha_w$  and  $C_w$  are the volumetric thermal expansion coefficient and the volumetric compressibility of pore water, respectively,  $V_w$  is the current volume of pore water.

Campanella and Mitchell [14] suggested that the clay mass would experience the same thermal volumetric strain as that of each mineral solid particle. In other words, the thermal expansion coefficient of the total soil mass is assumed equal to that of the mineral solid ( $\alpha_s$ ). Thereby, the volume change of clay mass due to temperature changes can be calculated by:

$$(dV)_{dT} = V \alpha_s dT \quad (6)$$

where  $V$  is the current volume of the total clay mass,  $V = V_s + V_w$ .

The volume change of the clay mass due to effective stress changes can be calculated by:

$$(dV)_{dp} = -VC_d dp' \quad (7)$$

where  $C_d$  is the volumetric compressibility of soil skeleton that is effective stress dependent but temperature independent.

Combining Eqs (1)-(7) and taking into account the Terzaghi's effective stress principle ( $p' = p - u$ ) gives the expressions for incremental volumetric strain and pore water pressure, respectively:

$$d\varepsilon_v = \frac{-dV}{V} = -(n\alpha_w + (1-n)\alpha_s)dT + n(C_w - C_s)du + (1-n)C_s dp \quad (8)$$

$$du = \frac{(C_d - (1-n)C_s)dp + n(\alpha_w - \alpha_s)dT}{(nC_w + C_d)} \quad (9)$$

where  $n = \frac{V_w}{V}$  is the Eulerian porosity, defined as the ratio of the current porous volume to the current soil volume.

### 3.2. Expressions after Lewis and Schrefler (1987)

The Darcy velocity of the water within the pore space of porous media is defined as:

$$\boldsymbol{\gamma} = -\frac{1}{\mu} \mathbf{k} \nabla (u + \rho_w g h) \quad (10)$$

where  $\mu$  is the dynamic viscosity of the water,  $\mathbf{k}$  is the absolute permeability matrix,  $u$  is the pore water pressure,  $\rho_w$  is the density of water,  $\nabla$  stands for the nabla operator,  $g$  is the gravity and  $h$  is the head above some arbitrary datum.

In the isotropic state, the total mean stress  $p$  is decomposed into a pore water pressure  $u$  and a mean effective stress  $p'$ . The rate of water accumulation can be attributed to:

(a) Rate of change of total volumetric strain:  $\frac{\partial \varepsilon_v}{\partial t}$ .

(b) Rate of change of the mineral solid volume due to changes of pore water pressure and temperature:  $(1-\phi) \left( \alpha_s \frac{\partial T}{\partial t} - C_s \frac{\partial u}{\partial t} \right)$ , where  $\phi = \frac{V_\phi}{V_0}$  is the Lagrangian porosity defined as the

ratio of the current porous volume to the initial clay volume,  $\alpha_s$  and  $C_s$  are the volumetric thermal expansion coefficient and the volumetric compressibility of mineral solid, respectively.

(c) Rate of change of the mineral solid volume due to changes of mean effective stress:  $-C_s \frac{\partial p'}{\partial t}$ .

(d) Rate of change of water density:  $\phi \left( -C_w \frac{\partial u}{\partial t} + \alpha_w \frac{\partial T}{\partial t} \right)$ .

The water mass balance equation under non-isothermal conditions, in combination with Darcy's law (Eq (10)) is given by:

$$\nabla^t (\rho_w \boldsymbol{\gamma}) = \text{rate of water accumulation} \quad (11)$$

Under undrained conditions, no flow occurs and  $\boldsymbol{\gamma} = \mathbf{0}$  holds. Thus, the rate of water accumulation is null, resulting in:



$$\frac{\partial \varepsilon_v}{\partial t} = -(\phi \alpha_w + (1-\phi) \alpha_s) \frac{\partial T}{\partial t} + (\phi C_w + (1-\phi) C_s) \frac{\partial u}{\partial t} + C_s \frac{\partial p'}{\partial t} \quad (12)$$

and

$$d\varepsilon_v = -(\phi \alpha_w + (1-\phi) \alpha_s) dT + \phi (C_w - C_s) du + C_s dp \quad (13)$$

The constitutive equation relating the effective stresses to the strains of the soil skeleton can be written as [38]:

$$dp' = K (d\varepsilon_v - \alpha_s dT - C_s du) \quad (14)$$

where  $K$  is the bulk modulus of soil skeleton.

Substituting Eq (13) into Eq (14) gives the expression for incremental pore water pressure:

$$du = \frac{(C_d - C_s) dp + (\phi \alpha_w - \phi \alpha_s) dT}{(C_d - C_s) + (\phi C_w - \phi C_s)} \quad (15)$$

where  $C_d = 1/K$  is the volumetric compressibility of soil skeleton.

With infinitesimal transformation, Eqs (13) and (15) can be written using Eulerian porosity  $n$ :

$$d\varepsilon_v = -(n \alpha_w + (1-n) \alpha_s) dT + n (C_w - C_s) du + C_s dp \quad (16)$$

$$du = \frac{(C_d - C_s) dp + n (\alpha_w - \alpha_s) dT}{(C_d - C_s) + n (C_w - C_s)} \quad (17)$$

### 3.3. Expressions after Coussy (2004)

The undrained heating process is analyzed and all the formulations are derived on the basis of thermo-poro-elastic theory. In the isotropic stress state and under non-isothermal condition, the total mean stress change ( $dp$ ) and Lagrangian porosity change ( $d\phi$ ) can be expressed by changes of volumetric strain ( $d\varepsilon_v$ ), pore water pressure ( $du$ ) and temperature ( $dT$ ), as follows:

$$dp = \frac{1}{C_d} d\varepsilon_v + b du + \frac{1}{C_d} \alpha_d dT \quad (18)$$

$$d\phi = -b d\varepsilon_v - \frac{1}{N} du + \alpha_\phi dT \quad (19)$$

with the Maxwell's symmetry condition given by:

$$b = \left( \frac{\partial p}{\partial u} \right)_{\varepsilon_v, T} = - \left( \frac{\partial \phi}{\partial \varepsilon_v} \right)_{u, T} \quad (20)$$

The volumetric compressibility of soil skeleton  $C_d$ , the Biot coefficient  $b$  and the volumetric thermal dilation coefficient of soil skeleton  $\alpha_d$  appearing in Eq (18) are defined as:

$$\frac{1}{C_d} = \left( \frac{\partial p}{\partial \varepsilon_v} \right)_{u, T}, \quad b = \left( \frac{\partial p}{\partial u} \right)_{\varepsilon_v, T}, \quad \alpha_d = - \left( \frac{\partial \varepsilon_v}{\partial T} \right)_{p, u} \quad (21)$$

The Biot coefficient  $b$ , Biot modulus  $N$  and the volumetric thermal expansion coefficient of pores  $\alpha_\phi$  appearing in Eq (19) are defined as:

$$b = -\left(\frac{\partial \phi}{\partial \varepsilon_v}\right)_{u,T}, \quad \frac{I}{N} = -\left(\frac{\partial \phi}{\partial u}\right)_{\varepsilon_v,T}, \quad \alpha_\phi = \left(\frac{\partial \phi}{\partial T}\right)_{\varepsilon_v,u} \quad (22)$$

Eqs (21)-(22) are partial differential equations and the subscripts indicate that the corresponding variables are kept constant, e.g. expression of  $1/C_d$  in Eq (21) corresponds to an isothermal drained compression test in which the pore water pressure and temperature are unchanged.

Considering the relations between the skeleton and mineral solid properties, the compatibility relations can be obtained:

$$\begin{aligned} b &= 1 - \frac{C_s}{C_d}, \quad \frac{I}{N} = (\phi - b)C_s \\ \alpha_d &= \alpha_s, \quad \alpha_\phi = (\phi - b)\alpha_s \end{aligned} \quad (23)$$

where  $C_s$  and  $\alpha_s$  are the volumetric compressibility coefficient and the thermal dilation coefficient of mineral solid, respectively.

In a saturated porous media, the current water mass ( $m_w$ ) per unit volume can be expressed as:

$$m_w = \rho_w \phi \quad (24)$$

Differentiating Eq (24) gives:

$$\frac{dm_w}{\rho_w} = d\phi + \phi \frac{d\rho_w}{\rho_w} \quad (25)$$

The state equation of water writes as follows:

$$\frac{d\rho_w}{\rho_w} = (C_w du - \alpha_w dT) \quad (26)$$

where  $C_w$  is the volumetric compressibility of water.

From Eqs (18)-(19), (23), (25)-(26), it gives:

$$\frac{dm_w}{\rho_w} = -(C_d - C_s)dp - ((\phi C_s - \phi C_w) - (C_d - C_s))du + (\phi \alpha_s - \phi \alpha_w)dT \quad (27)$$

Under undrained conditions, the mass of the fluid phase is constant and  $dm_w = 0$  holds. Thus, the expressions for incremental volumetric strain and pore water pressure from Eqs (18) and (27) can be obtained, as follows:

$$d\varepsilon_v = -(\phi \alpha_w + (1 - \phi) \alpha_s)dT + \phi(C_w - C_s)du + C_s dp \quad (28)$$

$$du = \frac{(C_d - C_s)dp + (\phi\alpha_w - \phi\alpha_s)dT}{(C_d - C_s) + (\phi C_w - \phi C_s)} \quad (29)$$

With infinitesimal transformation, Eqs (28) and (29) can be written as Eqs (16) and (17) using Eulerian porosity  $n$ .

### 3.4. Comparison and discussion

Comparison of the final expressions for pore water pressure changes, i.e. Eqs (9), (17) and (29), suggests that the expression proposed by Lewis and Schrefler [17] and Coussy [18] are the same but different from the one proposed by Campanella and Mitchell [14]. However, if the solid grain is assumed incompressible, i.e.  $C_s = 0$ , the three approaches unify.

The volume change of mineral solid due to the mean effective stress change is expressed as  $-C_s V_s dp'$  by Campanella and Mitchell [14] (see Eq (3)). This assumption may be questioned and requires further examination according to Ranjan *et al.* [24]. The mean effective stress acting on the mineral solid is  $dp'/(1-n)$ , and the corresponding volume change is given by:

$$(dV_s)_{dp'} = -(1-n)VC_s \frac{dp'}{1-n} = -VC_s dp' \quad (30)$$

Thus, the expression for the volume change of mineral solid due to the mean effective stress change now has the same form as the ones derived by Lewis and Schrefler [17] and Coussy [18].

Moreover, since a compressible mineral solid is considered by Campanella and Mitchell [14], Eq (7) for calculating the volume change of clay mass due to stress should be rewritten to consider also the volume change caused by isotropic compression of mineral solids by the pore water [38] as follows:

$$(dV)_{dp} = -VC_d dp' - VC_s du \quad (31)$$

Hence, using Eqs (30) and (31) in the approach of Campanella and Mitchell [14] provides the same expressions for the pore water pressure increment as that of Lewis and Schrefler [17] and Coussy [18].

The equations proposed by Campanella and Mitchell [14] can also be examined from a mechanical point of view. For a non-isothermal loading process, the basic governing equation under undrained condition (see Eq (1)) holds. However, it should be noted that:

$$V_s \alpha_s dT + V_w \alpha_w dT \neq V \alpha_s dT \quad (32)$$

i.e.

$$(dV_s)_{dT} + (dV_w)_{dT} \neq (dV)_{dT} \quad (33)$$

Thus:

$$(dV_s)_{dp} + (dV_w)_{dp} \neq (dV)_{dp} \quad (34)$$

This means that each term in Eqs (33) and (34) that describe the temperature and stress effects on the clay volume change respectively are not defined in a decoupled manner and thereby do not work independently. It appears then necessary to present the equations in a different form within the framework of Campanella and Mitchell [14], where each term is defined in a decoupled manner to highlight more clearly their physical meaning; this is possible because  $u$ ,  $p$  and  $T$  are independent variables that define the state of the system during reversible processes. The non-isothermal loading process for the whole clay mass can be further divided into two processes: (i) a heating one with a temperature change  $dT$  and (ii) an isothermal loading one with a mean stress change  $dp$ . In a heating process (process i) under undrained condition, a temperature increase  $dT$  generates a pore water pressure ( $du_1$ ), thus changing the mean effective stress ( $dp'_1 = -du_1$ ). During this process, the volume changes of pore water, mineral solid and the whole mass due to temperature can be expressed as:

$$(dV_w)_{dT} = V_w \alpha_w dT - V_w C_w du_1 \quad (35)$$

$$(dV_s)_{dT} = V_s \alpha_s dT - V_s C_s du_1 - VC_s dp'_1 \quad (36)$$

$$(dV)_{dT} = V \alpha_s dT - VC_s du_1 - VC_d dp'_1 \quad (37)$$

In an isothermal loading process (process ii) under undrained condition, pore water pressure ( $du_2$ ) is generated by the mean stress changes ( $dp$ ). Accordingly, the mean effective stress changes ( $dp'_2 = dp - du_2$ ). During this process, the total pore pressure increment is  $du = du_1 + du_2$ . The volume change of pore water, mineral solid and the whole mass due to pressure can be expressed as:

$$(dV_w)_{dp} = -V_w C_w du_2 \quad (38)$$

$$(dV_s)_{dp} = -V_s C_s du_2 - VC_s dp'_2 \quad (39)$$

$$(dV)_{dp} = -VC_s du_2 - VC_d dp'_2 \quad (40)$$

Substituting Eqs (35)-(40) into Eq (1) leads to the same expressions as that of Lewis and Schrefler [17] and Coussy [18], showing the compatibility among the above three different approaches.

## 4. Thermo-elasto-plastic constitutive modeling

### 4.1 Thermo-elasto-plastic framework for undrained conditions

The thermo-elasto-plastic framework for clays under undrained conditions was elaborated by extending the thermo-hydro-mechanical equations in the elastic state by Coussy [18] (see section 3.3) to the elasto-plastic state. As pointed out by Coussy [18], plastic evolutions are induced by the irreversible relative sliding of solid grains (or particles) forming the solid matrix of clays. Thus, the plastic change of the solid part is negligible, while the plastic strain of solid skeleton due to temperature and stress changes should be considered. The skeletal thermal strain is assumed to be entirely elastic. The mechanical stress-strain relation is elasto-plastic, considering the skeleton modulus changes due to both temperature and stress. Equation (18) for the total strain is extended for this purpose:

$$d\boldsymbol{\varepsilon} = \mathbf{C}(d\boldsymbol{\sigma} - \mathbf{m}^t du) - \frac{I}{3} \mathbf{m}^t \alpha_d dT + \frac{I}{3} \mathbf{m}^t C_s du \quad (41)$$

where  $\mathbf{C}$  is the elasto-plastic compliance matrix of the soil skeleton,  $C_s$  is the volumetric compressibility coefficient of mineral solid and  $\mathbf{m}^t$  denotes the identity matrix.

The relation of stress-strain-temperature increments can be obtained from Eq (41):

$$d\boldsymbol{\sigma} = \mathbf{D}d\boldsymbol{\varepsilon} + \frac{I}{3} \mathbf{D} \mathbf{m}^t \alpha_d dT + \left( \mathbf{m}^t - \frac{I}{3} \mathbf{D} \mathbf{m}^t C_s \right) du \quad (42)$$

where  $\mathbf{D} = \mathbf{C}^{-1}$  denotes the elasto-plastic stiffness matrix of the soil skeleton.

Consider the isotropic stress state, the expression of the total mean stress change ( $dp$ ) and lagrangian porosity change ( $d\phi$ ) for the thermo-elasto-plasticity state are derived:

$$dp = \frac{I}{C'_d} d\varepsilon_v + b' du + \frac{I}{C'_d} \alpha_d dT \quad (43)$$

$$d\phi = -b' d\varepsilon_v - \frac{I}{N} du + \alpha_\phi dT \quad (44)$$

where  $b' = I - \frac{C_s}{C'_d}$  with  $C'_d$  denoting the elasto-plastic compressibility of the soil skeleton.

Proceeding as in Section 3.3, the thermo-elasto-plastic expressions of volumetric strain in the undrained heating process is same as Eq (28) and pore water pressure can be obtained:

$$du = \frac{(C'_d - C_s) dp + \phi(\alpha_w - \alpha_s) dT}{(C'_d - C_s) + \phi(C_w - C_s)} \quad (45)$$

Since the constitutive equations are developed from the formulations proposed by Coussy [18], the compressibility of mineral solid part is included. This is different from the conventional

constitutive models for clays under undrained conditions. Thus, it is worthwhile to examine the effects of  $C_s$  on the clay response. For this purpose, a parametric study on  $C_s$  has been performed by numerical simulation of an undrained heating test of natural Boom Clay sample from 25 °C to 65 °C under a constant total stress of 3.25 MPa. An initial back pressure of 1 MPa is applied.  $C_s$  varies from  $2 \times 10^{-3}$  to 0 MPa<sup>-1</sup>. Note that the value  $C_s = 2 \times 10^{-6}$  MPa<sup>-1</sup> is the actual value according to McTigue [25].

All the other parameters involving the parameters for soil skeleton (see Table 1) and the variable volumetric thermal expansion coefficient of pore water are adopted (see Eq (61)).

**Table 1** Numerical simulations of an undrained heating test with different values of  $C_s$ .

Simulation test	$C_s$ (MPa <sup>-1</sup> )	$C'_d$ (MPa <sup>-1</sup> )*	$b' = 1 - C_s/C'_d$
A	$2 \times 10^{-3}$	$5.4 \times 10^{-3}$	0.63000
B	$2 \times 10^{-4}$	$5.4 \times 10^{-3}$	0.963000
C	$2 \times 10^{-5}$	$5.4 \times 10^{-3}$	0.99630
D	$2 \times 10^{-6}$	$5.4 \times 10^{-3}$	0.99963
E	0	$5.4 \times 10^{-3}$	1

\* value for the initial state with  $p' = 2.3$  MPa and  $T = 25$  °C.

Fig. 2 presents the results of this parametric study. Taking simulation E (i.e.  $C_s = 0$ ) as the reference calculation, it is found that varying  $C_s$  from 0 to  $2 \times 10^{-4}$  (MPa<sup>-1</sup>), which induces initial values of coefficient  $b'$  ranging from 1 to 0.96300 respectively, has a negligible effect on the simulation results (Simulation B, C and D). However, with  $b' = 0.63$ , a significant effect is observed when  $C_s$  reaches  $2 \times 10^{-3}$  (MPa<sup>-1</sup>) (Simulation A). It is worth noting that the compressibility of solid grain ( $C_s$ ) and the soil skeleton ( $C'_d$ ) in saturated porous rock and concrete are of the same order of magnitude, i.e., the value of  $b'$  may be as low as 0.5, and the  $C_s$  effect could not be neglected. On the contrary,  $C_s$  is much smaller than  $C'_d$  for most clays, i.e.,  $b' \approx 1$ , and the compressibility of solid grain can be neglected in this case (i.e.  $C_s = 0$ ) [14, 26]. In other words, the following incremental stress-strain-temperature relation can be applied with  $C_s = 0$ :

$$d\sigma = \mathbf{D}d\epsilon + \mathbf{m}'du + \frac{1}{3}\mathbf{D}\mathbf{m}'\alpha_d dT \quad (46)$$

with the volumetric strain in the undrained heating process:

$$d\epsilon_v = -(\phi\alpha_w + (1-\phi)\alpha_s)dT + \phi C_w du \quad (47)$$

It is worth noting that Eq (47) developed from Coussy [18] implies an undrained heating condition with a constant water mass content per initial unit volume. Equations (46) and (47) allow the pore water pressure calculation and undrained behavior prediction. The variation of

the elasto-plastic stiffness tensor of the soil skeleton, i.e.  $\mathbf{D}$  in Eq (46) can be obtained from any thermo-mechanical model developed in drained conditions.

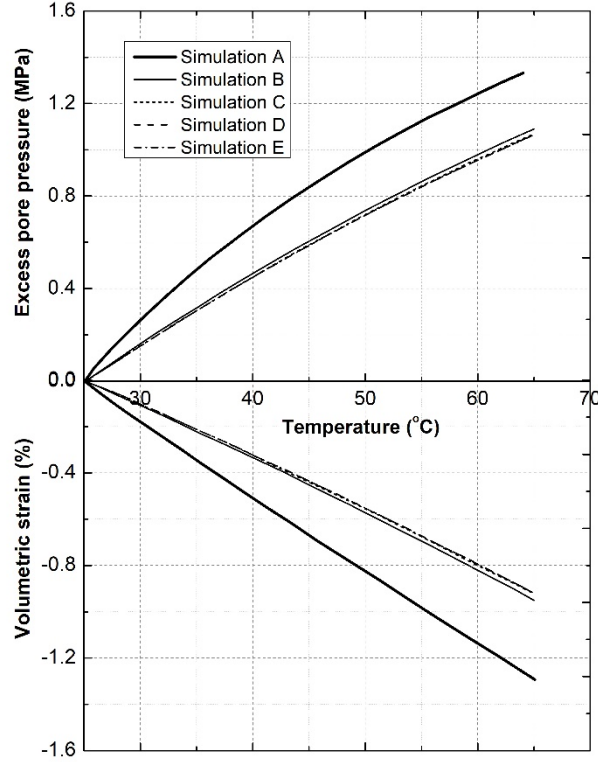


**Fig. 2** Numerical simulation results with different  $C_s$  values.

#### 4.2 A two-surface thermo-mechanical model

Hong *et al.* [23] developed a two-surface thermo-mechanical model, namely TEAM model to reproduce the drained thermo-elasto-plastic behavior, in which the elastoplastic stiffness tensor  $\mathbf{D}$  for the soil skeleton is defined. An isothermal version of this two-surface elastoplastic constitutive model was presented in [40]. In that work, the advantages of the intrinsic features of this two-surface model compared to a conventional Modified Cam Clay model were discussed. Of course, these advantages remain valid for the thermal extensions of these models. TEAM model itself is now extended in a straightforward manner to account for undrained conditions. The validation of such an extension is conveniently performed at the material point level. In the present section, TEAM model is briefly reviewed. It is formulated in the triaxial stress space considering non-isothermal conditions, i.e. in  $(p'-q-T)$  space with  $q$  being the deviator stress.

##### 4.2.1 Elastic behaviour

The elastic strain increment is decomposed into volumetric and shear components,  $d\varepsilon_v^e$  and  $d\varepsilon_s^e$ , the shear strain being assumed to be temperature independent. Thus, the elastic behavior is expressed as follows:

$$d\varepsilon_v^e = \frac{\kappa dp'}{v_0 p'} - \alpha_d dT; \quad d\varepsilon_s^e = \frac{dq}{3G} \quad (48)$$

where  $\kappa$  is the elastic slope in  $(v, \ln p')$  space, assumed temperature independent,  $v_0$  is the initial specific volume,  $\alpha_d$  is the drained thermal volumetric expansion coefficient of soil skeleton which is assumed constant;  $G$  is the shear modulus.

#### 4.2.2 Plastic behavior

Following the thermo-mechanical model of Cui *et al.* [8], the conventional yield surfaces - namely Yield surfaces-comprising LY (loading yield limit) and TY (thermal yield limit) are introduced (see Fig. 3): the evolution of LY is controlled by the pre-consolidation pressure ( $\bar{p}'_{c0}$ ) at a reference temperature ( $T_0$ ), and the plastic volumetric strain in normally consolidated state depends on the evolution of LY; TY is used to govern the thermal plastic behavior inside LY. To achieve a wide variety of yield surface shapes in  $p'-q$  plane, a generalized yield surface proposed by McDowell and Hau [27] is adopted for LY at a given temperature  $T$ . The yield surface LY in  $(p'-q-T)$  space is given as follows:

$$f_{LY} \equiv q^2 + \frac{M_f^2}{1-k_f} \left( \frac{p'}{\bar{p}'_{cT}} \right)^{2/k_f} \bar{p}'_{cT}^2 - \frac{M_f^2 p'^2}{1-k_f} = 0 \quad (49)$$

with

$$\bar{p}'_{cT} = \bar{p}'_{c0} \exp[-\alpha_0(T - T_0)] \quad (50)$$

where  $M_f$  and  $k_f$  are parameters to specify the shape of LY in  $(p', q)$  plane at a given temperature;  $\bar{p}'_{c0}$  and  $\bar{p}'_{cT}$  are defined as the apparent pre-consolidation pressures at a reference temperature  $T_0$  and the actual temperature  $T$  respectively;  $\alpha_0$  controls the curvature of LY.

The expression of TY is defined as follows:

$$f_{TY} \equiv T - \bar{T}_c + \frac{1}{\beta} \ln \left( \frac{p'}{p'_{ref}} \right) = 0 \quad (51)$$



where  $p'_{ref}$  is a reference pressure and taken equal to the atmospheric pressure (0.1 MPa);  $\bar{T}_c$  and  $T$  are the yield temperature corresponding to  $p'_{ref}$  and  $p'$  respectively;  $\beta$  is a parameter governing the shape of TY curve.

To account for a smooth transition from the elastic state to the elastoplastic state, Inner yield surfaces comprising ILY (inner loading yield limit) and ITY (inner thermal yield limit) are introduced with the hardening variables  $T_c$  and  $p'_{c0}$  respectively. As illustrated in Fig. 3, the variables  $T_c$  and  $p'_{c0}$  are analogous to  $T_c$  and  $\bar{p}'_{c0}$  respectively. The introduction of these inner yield surfaces allows the progressive generation of irreversible deformation before the corresponding formal yield surfaces are reached by the point representing the material state of stress and temperature, thus inducing a smooth transition in the vicinity of the yield limit and more realistic simulations.

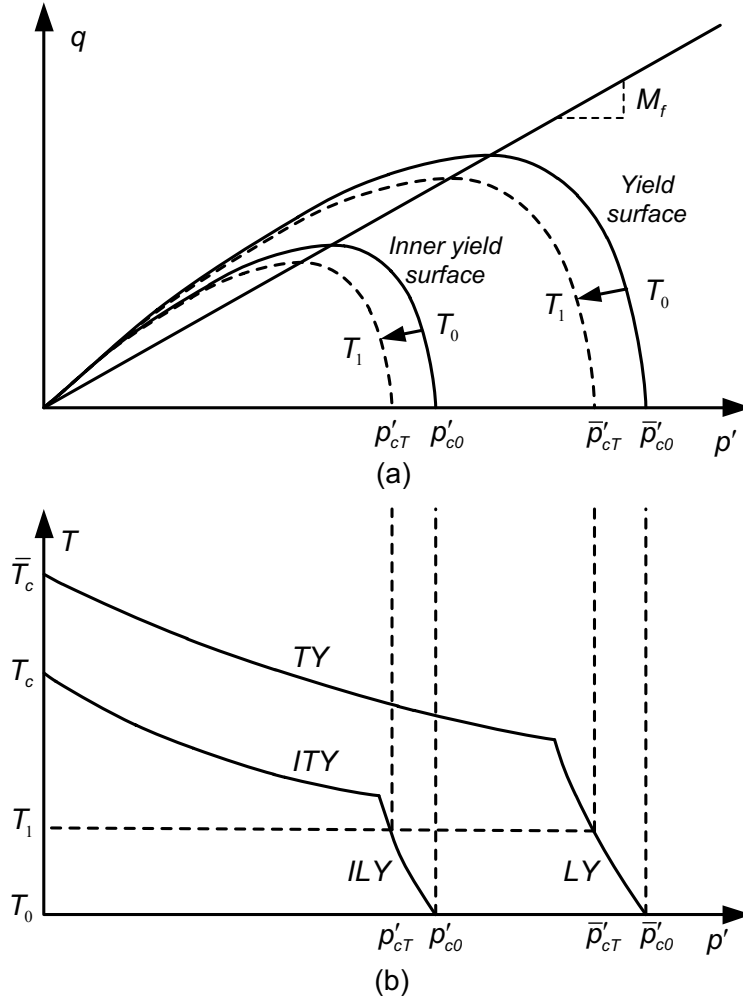


**Fig. 3** Yield locus in (a):  $(p'-q)$  plane at two different temperatures (with  $T_1 > T_0$ ); and (b):  $(p'-T)$  plane.

Two scalars are introduced for each mechanism, given by the ratio of the size of a given Yield surface to that of the corresponding Inner yield surface. Their values are always smaller than or

equal to unity. Thus, the ratios  $r^{LY}$  and  $r^{TY}$  for LY (loading yield limit) and TY (thermal yield limit) plastic mechanisms are respectively defined as:

$$r^{LY} = \frac{p'_{c0}}{\bar{p}'_{c0}}; \quad r^{TY} = \frac{T_c}{\bar{T}_c} \quad (52)$$

ILY is chosen as homologous to LY with respect to the origin in  $(p'-q-T)$  space; the definition of ILY is therefore given by:

$$f_{ILY} \equiv q^2 + \frac{M_f^2}{1-k_f} \left( \frac{p'}{r^{LY} \bar{p}'_{cT}} \right)^{2/k_f} (r^{LY} \bar{p}'_{cT})^2 - \frac{M_f^2 p'^2}{1-k_f} = 0 \quad (53)$$

Similarly, the expression of ITY is defined as follows:

$$f_{ITY} \equiv T - r^{TY} \bar{T}_c + \frac{1}{\beta} \ln \left( \frac{p'}{p'_{ref}} \right) = 0 \quad (54)$$

The hardening parameters  $r^{LY}$  and  $\bar{p}'_{c0}$  are defined to control the size of ILY and LY, respectively. The internal variable increment  $d\bar{p}'_{c0}$  depends on the volumetric plastic strain increment associated with LY plastic mechanism. Furthermore, experimental observations in Cui *et al.* [8] show that LY curve hardens when TY is activated while activation of LY does not produce any hardening of TY, so that a unidirectional coupling between TY and LY is taken into account. Therefore, the plastic strain increment associated with TY plastic mechanism and LY plastic mechanism will also generate an increase of  $\bar{p}'_{c0}$  and the plastic hardening law for  $\bar{p}'_{c0}$  can be defined as:

$$d\bar{p}'_{c0} = \frac{v_0}{\lambda - \kappa} \bar{p}'_{c0} (d\varepsilon_{vTY}^p + d\varepsilon_{vLY}^p) \quad (55)$$

where  $d\varepsilon_{vTY}^p$  and  $d\varepsilon_{vLY}^p$  are the plastic volumetric increments associated with TY mechanism and LY mechanism, respectively.

To describe the variation of the hardening modulus upon thermo-mechanical loading as ILY is activated, the evolution law of  $r^{LY}$  can be defined as:

$$dr^{LY} = \frac{v_0}{\lambda - \kappa} s^{LY} (1 - r^{LY}) (d\varepsilon_{vTY}^p + d\varepsilon_{vLY}^p + A_d d\varepsilon_{sLY}^p) \quad (56)$$

where  $s^{LY}$  is a material constant used to control the rate at which ILY approaches LY and thus the evolution of the slope of the stress/temperature-strain curve inside LY can be described.  $A_d$  is a parameter that controls the contribution of shear plastic strain  $d\varepsilon_{sLY}^p$  to soil hardening.

Experimental results show that the thermally induced plastic strain on TY is dependent on the given stress state (OCR effect). Thus, the hardening laws for TY and ITY are respectively defined as:

$$d\bar{T}_c = \frac{v_0}{(\lambda - \kappa)\alpha_0} f(OCR) d\varepsilon_{vTY}^p \quad (57)$$

with the function  $f(OCR)$  reading:

$$f(OCR) = 1 + s^{LY} (1 / r^{LY} - 1) \quad (58)$$

Similarly, to describe a smooth elasto-plastic transition as ITY is activated,  $r^{TY}$  is defined as follows:

$$dr^{TY} = \frac{v_0}{(\lambda - \kappa)\alpha_0 \bar{T}_c} f(OCR) s^{TY} (1 - r^{TY}) d\varepsilon_{vTY}^p \quad (59)$$

where  $s^{TY}$  is a material constant controlling the rate at which ITY approaches TY along thermo-mechanical loading paths and thus the evolution of the slope of the stress/temperature-strain curve inside TY can be described.

A non-associated flow rule in the case of triaxial compression is given with the following dilation ratio:

$$d = \frac{d\varepsilon_{vLY}^p}{d\varepsilon_{sLY}^p} = \frac{M_g^2 - \eta^2}{k_g \eta} \quad (60)$$

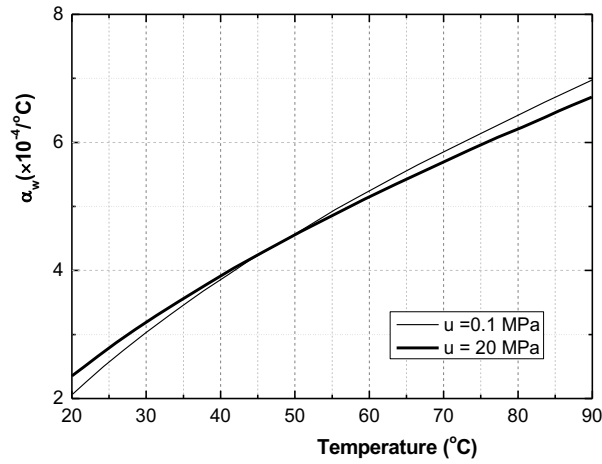
where  $M_g$  is the slope of the critical state line in  $(p', q)$  plane;  $\eta$  is the stress ratio  $q/p'$ ;  $k_g$  is a parameter used to specify the ratio between plastic volumetric strain increment and plastic shear strain increment.  $k_g = 2$  would lead to the flow rule of Modified Cam Clay model.

## 5. Determination of the thermo-hydro-mechanical parameters

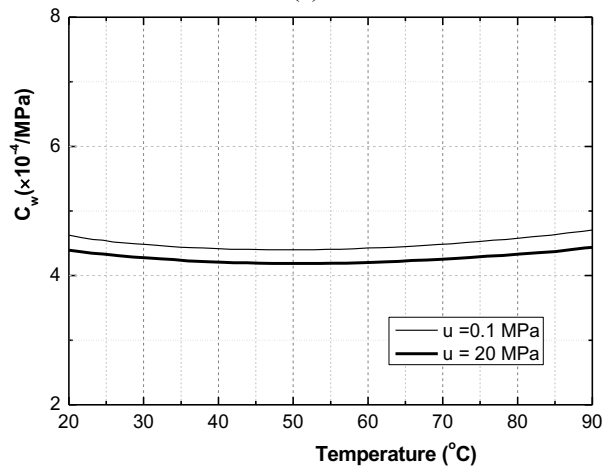
For the undrained behavior prediction, the calculation requires determining the parameters involving the soil skeleton (i.e, TEAM model) and these parameters can be determined according to their physical meaning. More details can be found in the work of Hong [23]. In addition, it is necessary to determine the hydro-mechanical parameters including the volumetric thermal expansion coefficients of mineral solid and pore water ( $\alpha_s$  and  $\alpha_w$ , respectively) as well as the compressibility coefficient of pore water ( $C_w$ ). The volumetric compressibility of mineral solid  $C_s$  can be neglected ( $C_s = 0$ ) in the case of clayey soils as discussed in Section 4.1.

The volumetric thermal expansion coefficient of solid ( $\alpha_s$ ) can be determined using the data from a physical handbook for the substances similar to the clay minerals, as recommended by Campanella and Mitchell [14]. In another way, since the values of  $\alpha_s$  and the volumetric thermal expansion coefficient of the soil skeleton ( $\alpha_d$ ) are equal (see Equation(23)),  $\alpha_s$  can take the value of  $\alpha_d$ , which can be calibrated from the cooling stages of a drained heating-cooling test in  $(\varepsilon_v-T)$  plane.

As described in the international-standard IAPWS-IF97 steam tables, the volumetric thermal expansion coefficient and compressibility of pore water,  $\alpha_w$  and  $C_w$ , vary with temperature and pressure [28, 29]. Fig. 4 presents the values of  $\alpha_w$  and  $C_w$  for the considered range of temperatures (from 20 °C to 90 °C) and pressures (at 0.1 MPa, namely atmospheric pressure and 20 MPa) [1]. It shows that  $\alpha_w$  varies significantly with temperature and less with pressure, while  $C_w$  varies in a small range [ $4.6 \times 10^{-4}$ ;  $4.8 \times 10^{-4}$ ] ( $\text{MPa}^{-1}$ ) for the considered temperature and pressure ranges.



(a)



(b)

**Fig. 4** Variation of properties of pore water with temperature and pressure: (a) volumetric thermal expansion coefficient  $\alpha_w$ ; (b) compressibility  $C_w$ .

The thermal expansion coefficient of pore water  $\alpha_w$  can be approximated by the following function involving the current pore pressure and temperature [20]:

$$\alpha_w(T, u) = x_0 + (x_1 + y_1 T) \ln(mu) + (x_2 + y_2 T) (\ln(mu))^2 \quad (61)$$

where parameters  $x_0$ ,  $x_1$ ,  $x_2$ ,  $y_1$ ,  $y_2$  and  $m$  are determined by fitting the data in Fig. 4 (a):  $x_0 = 4.2 \times 10^{-4} \text{ }^\circ\text{C}^{-1}$ ,  $x_1 = 5.7 \times 10^{-5} \text{ }^\circ\text{C}^{-1}$ ,  $x_2 = 2.4 \times 10^{-6} \text{ }^\circ\text{C}^{-1}$ ,  $y_1 = -1.3 \times 10^{-6} \text{ }^\circ\text{C}^{-2}$ ,  $y_2 = -5.6 \times 10^{-8} \text{ }^\circ\text{C}^{-2}$ ,  $m = 0.0001 \text{ MPa}^{-1}$ .

However, in several THM models [14, 34, 35], the thermal expansion coefficient of pore water  $\alpha_w$  is often regarded as a constant (normally  $3.3 \sim 4.5 \times 10^{-4} \text{ }^\circ\text{C}^{-1}$  in the temperature range of  $16.5 \sim 40 \text{ }^\circ\text{C}$ ) for simplicity. In the following sections, the undrained heating test is conducted in the temperature range of  $25 \sim 65 \text{ }^\circ\text{C}$ ,  $21 \sim 92 \text{ }^\circ\text{C}$ ,  $22 \sim 95 \text{ }^\circ\text{C}$ , respectively. Therefore, the effects of variable  $\alpha_w(T, u)$  and constant  $\alpha_w (5 \times 10^{-4} \text{ }^\circ\text{C}^{-1})$  under undrained heating conditions are also investigated in the following sections.

Furthermore, the volumetric compressibility of pore water is assumed to be equal to the one of bulk water in the absence of any relevant experimental data.

## 6. Experimental validation

The capability of the proposed model for describing the undrained behavior of saturated clays has been validated based on some undrained heating tests on natural Boom Clay and reconstituted Pontida Clay.

### 6.1 Undrained heating test under isotropic stress conditions on natural Boom Clay

An undrained heating test on natural Boom Clay was performed by Monfared *et al.* [13] using a temperature-controlled triaxial equipment. The sample was saturated under the in-situ mean effective stress of 2.25 MPa and a back pressure of 1 MPa. Then the sample was submitted to a heating process from  $25 \text{ }^\circ\text{C}$  to  $65 \text{ }^\circ\text{C}$  under undrained condition at a constant total stress of 3.25 MPa. The heating rate was  $1 \text{ }^\circ\text{C}/\text{hour}$ . The pore water pressure change was monitored by a pressure transducer at the bottom of the sample and the volume change of the sample was monitored by LVDT transducers installed on the specimen. The experimental results are shown in Fig. 5.

The volumetric thermal expansion coefficient of solid  $\alpha_s$  is estimated to be  $5 \times 10^{-5} \text{ }^\circ\text{C}^{-1}$ , which is equal to the value of  $\alpha_d$  by Hong *et al.* [2]. The equality of these two coefficients can easily be demonstrated in the case of a homogeneous solid phase [41]. A constant value for the volumetric compressibility of pore water,  $C_w = 4.7 \times 10^{-4} \text{ MPa}^{-1}$ , is chosen since it does not vary significantly for the considered temperature and pressure ranges, as seen previously. For comparison purposes, a variable  $\alpha_w$  of pore water calculated using Eq (61) and a constant value of  $\alpha_w$  ( $5 \times 10^{-4} \text{ }^\circ\text{C}^{-1}$ ) are used in the simulations. For Eq (61), the required physical parameters were not measured in this test and thus are calibrated from other studies[1]. The other parameters of TEAM model for Boom clay's elastoplastic behavior were evaluated on the basis of drained tests described in Hong [23] and presented in Table 2.

**Table 2** Material parameters of TEAM model for soil skeleton elastoplasticity

	Natural Boom Clay	reconstituted Pontida Clay
$\lambda$	0.180	0.103
$\kappa$	0.020	0.016
$\alpha_d (1/^\circ\text{C})$	0.00005	0.00005
$\alpha_0 (1/^\circ\text{C})$	0.005	0.0035
$r_0^{LY} *$	0.33 / 1	1.0
$\bar{p}'_{c00} (\text{MPa}) *$	6 / 6	0.1
$s^{LY}$	8	10
$\beta$	0.021	0.072
$r_0^{TY} *$	0.76 / 1	0.18
$\bar{T}_{c0} (^\circ\text{C}) *$	216 / 244	110
$s^{TY}$	1.2	12
$M_f$	0.87	-
$k_f$	0.7	-
$\nu$	0.3	-
$M_g$	0.87	-
$k_g$	0.9	-
$A_d$	0.1	-

‘-’ means these parameters are irrelevant to simulation in the present study.

‘\*’ the former value is for Section 6.1 and the latter is for Section 6.2.

Fig. 5 presents excess pore water pressure and volumetric strain simulated with the variable and constant volumetric thermal expansion coefficients of pore water. One can easily find that constant thermal expansion coefficient ( $5 \times 10^{-4} \text{ }^\circ\text{C}^{-1}$ ) is much larger than the actual values of

pore water before around 57 °C and slightly smaller after 57 °C in Fig.4(a). However, comparison of the obtained results with the experimental data shows that the prediction results with the constant volumetric thermal expansion coefficient ( $5 \times 10^{-4} \text{ }^\circ\text{C}^{-1}$ ) agree better with the experimental results than the variable value of pore water. This phenomenon can be attributed to two possible reasons. One is the material parameters of TEAM model which are calibrated in drained tests. The other is that there is an amount of adsorbed water in pores of low-porosity clays (e.g. Boom clay, Cox) which has sharply changed the thermal expansion behavior of pore water as described by Baldi et al [20]. However, this assumption requires more macro-experimental observations and further insights from a microscale point of view.

Fig. 6 presents the effective stress path of undrained isotropic heating test from 25 °C to 65 °C with  $\alpha_w(T, u)$ . It indicates that the mean effective stress decreases faster than ILY, but slower than ITY so that plastic strains occur. During the heating stage, the mean effective stress will remain on ITY while it decreases slower than ITY.

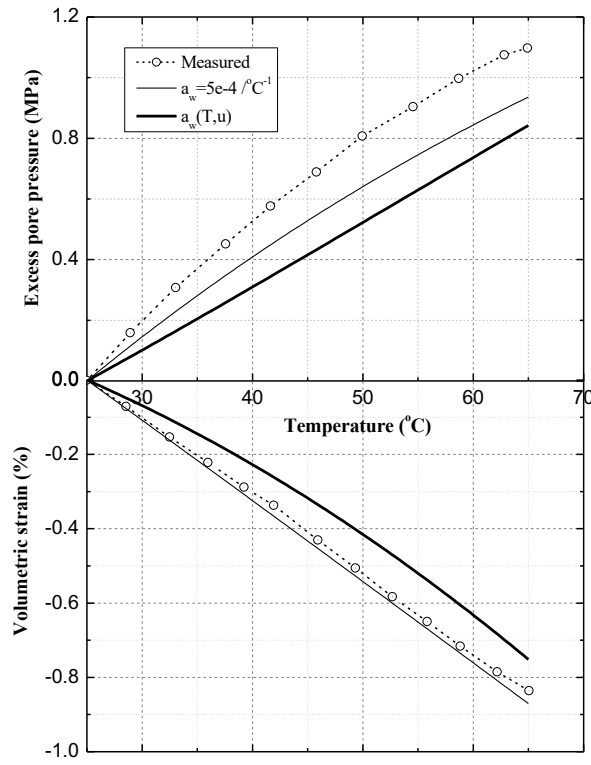


**Fig. 5** Undrained isotropic heating test on natural Boom clay from 25 °C to 65 °C

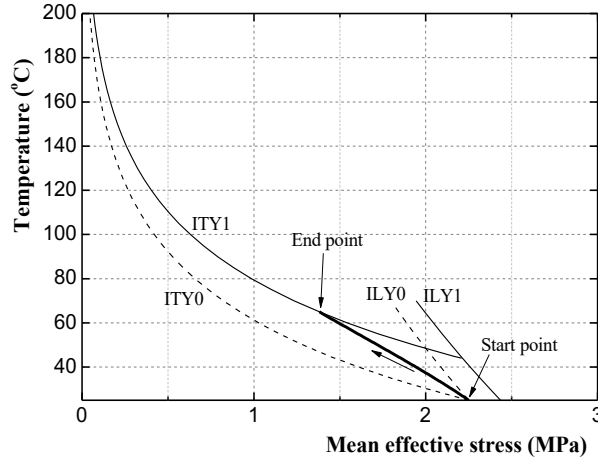


**Fig. 6** Effective stress path of undrained isotropic heating test from 25 °C to 65 °C with  $\alpha_w(T, u)$

### 6.2 Undrained heating test under constant deviatoric stress conditions on natural Boom Clay

An undrained heating test in deviatoric stress conditions on natural Boom Clay was performed after an undrained triaxial compression to a constant deviatoric stress conditions in a temperature-controlled triaxial equipment, as reported by Hueckel *et al.* [12]. The sample was first isotropically consolidated and then gradually subjected to a deviatoric stress under undrained condition. When the target deviatoric stress ( $q \approx 2.3$  MPa) was attained, the sample was left at room temperature of 22 °C for 48 hours before the undrained heating stage from 22 °C to 92 °C in controlled temperature steps. The experimental results are presented in Fig. 7. The parameters of TEAM model for Boom clay's elastoplastic behavior were selected in Table 2. Note that Boom clay's stress states are different between Section 6.1 (OCR=3) and Section 6.2 (OCR=1). As a consequence, the four state parameters ( $r_0^{LY}$ ,  $\bar{p}'_{c00}$ ,  $r_0^{TY}$ ,  $\bar{T}_{c0}$ ) should be updated, while the other 13 parameters remain the same.

Fig. 7 depicts the effective stress path and excess pore pressure assuming variable and constant thermal expansion coefficients for the pore water. During the undrained heating stage, excess pore pressure would build up and the mean effective stress would decrease towards the critical state line (CSL), eventually leading to thermal failure. This phenomenon is well captured by TEAM model. At the beginning of the heating process, the effective stress-temperature state ( $T$ - $p'$ - $q$ ) is assumed to lie on the Inner Yield surface. ILY decreases faster than the mean effective stress, so plasticity occurs before 35 °C. Between 35 °C and about 80 °C, the effective stress-temperature path ( $T$ - $p'$ - $q$ ) moves inside the Inner Yield surface and the response is purely elastic. Then the continuous heating makes the effective stress-temperature path ( $T$ - $p'$ - $q$ ) touch ITY and a plastic response reappears. Eventually, the effective stress-



temperature path ( $T$ - $p'$ - $q$ ) would stop on the CSL, as shown in Fig. 7(a) and Fig. 7(c). Excess pore pressure prediction using constant thermal expansion coefficient ( $5 \times 10^{-4} \text{ }^\circ\text{C}^{-1}$ ) is slightly larger than using a variable value. Compared with the constant value ( $5 \times 10^{-4} \text{ }^\circ\text{C}^{-1}$ ), the model with the variable value has a tendency of building up less excess pore pressure at low temperature, but more excess pore pressure at high temperature.

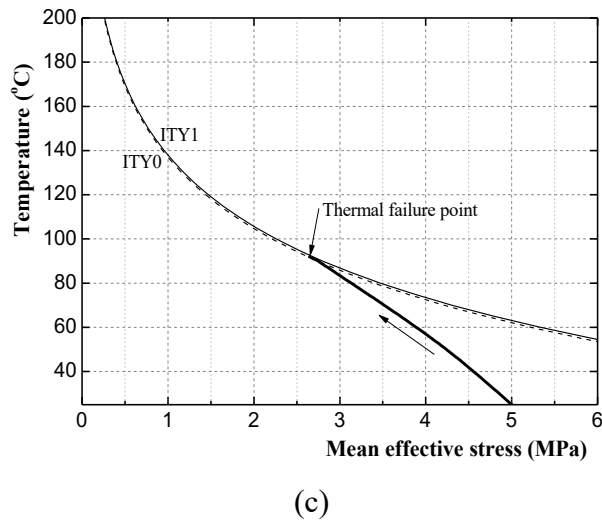
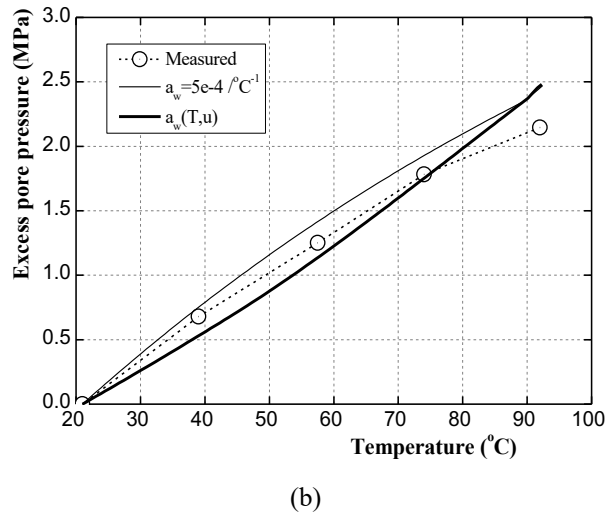
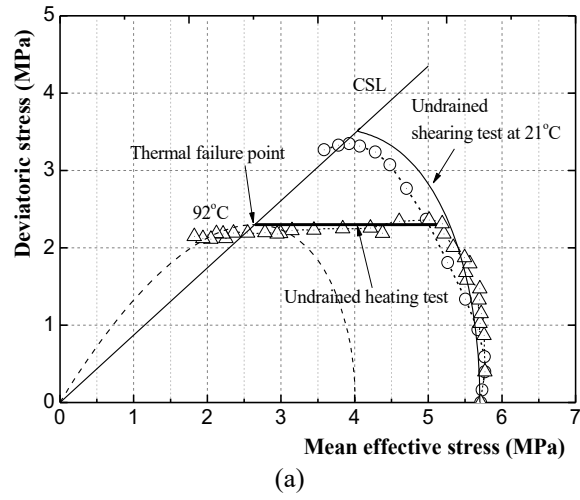


**Fig. 7** Undrained heating test under constant deviatoric stress condition from 21 °C to 92 °C: (a)  $(p', q)$  plane; (b) excess pore pressure vs temperature; (c)  $(p', T)$  plane with  $\alpha_w(T, u)$

### 6.3 Undrained heating test under isotropic conditions on reconstituted Pontida Clay

Hueckel *et al.* [33] reported the results of undrained heating-cooling tests on reconstituted Pontida Clay. From an initial mean effective stress of 2.5 MPa, the sample was submitted to a heating-cooling cycle from 22 °C to 65 °C and back to 22 °C, then a heating to 95 °C under a constant total isotropic stress. The experimental results are shown in Fig. 8.  $\alpha_s$  is  $5 \times 10^{-5}$  (1/°C) same as  $\alpha_d$ , which was calibrated from a drained heating test [2]. As done in Section 6.1,  $C_w = 4.7 \times 10^{-4}$  MPa<sup>-1</sup> is adopted for both cases. The variable  $\alpha_w$  calculated using Eq (61) and a constant value of  $\alpha_w$  ( $5 \times 10^{-4}$  °C<sup>-1</sup>) are used for pore waters. Other parameters of TEAM model for Pontida clay were calibrated in drained heating conditions from Hong [23] and presented in Table 2.

The simulation results of excess pore water pressure are compared with the experimental data in Fig. 8. In the heating-cooling phase from 22 °C to 65 °C (Fig. 9(a)) and back to 22 °C (Fig. 9(b)), irreversible pore water pressure change is observed, and this behavior is well captured by the proposed model. The initial effective stress-temperature state  $(T-p')$  is assumed to lie on ILY. During the heating stage, the mean effective stress will decrease with temperature due to the generation of excess pore pressure. The response is purely elastic and equivalent to a mechanical unloading before the effective stress-temperature path  $(T-p')$  reaches ITY plastic mechanism. With the plastic hardening of ITY, excess pore water pressure is increased while the loading state remains on the ITY surface, which happens while ITY decreases faster than the mean effective stress. One should also note that if mean effective stress decreases faster than ITY, the effective stress-temperature path  $(T-p')$  would move inside ITY and the behavior would remain purely elastic [39]. Then during the cooling stage, the response is purely elastic with a decrease of the pore water pressure. Thereby, an irreversible excess pore water pressure is predicted after the heating-cooling cycle because of the plastic regime attained during the heating stage. The model prediction fits experimental data very well. During the re-heating (Fig. 9(c)), the clay response is firstly elastic and then elasto-plastic after the  $T-p'$  loading path reaches ITY surface again. The irreversible response of the excess pore water pressure upon this heating-cooling process justifies the introduction of a thermal yield mechanism, such as the ITY plastic mechanism in a complete thermo-mechanical model.

On the other hand, the variable value of volumetric thermal expansion coefficient of pore water varies three times from 22 °C to 95 °C. It can sharply influence the prediction of excess pore water pressure. Compared with the constant value ( $5 \times 10^{-4} \text{ } ^\circ\text{C}^{-1}$ ), the model predicts less pore pressure accumulation under the thermal cycle from 22 °C to 65 °C and back to 22 °C. From heating phase from 65 °C to 95 °C, the model predicts more pore pressure buildup with the variable value than the constant one.

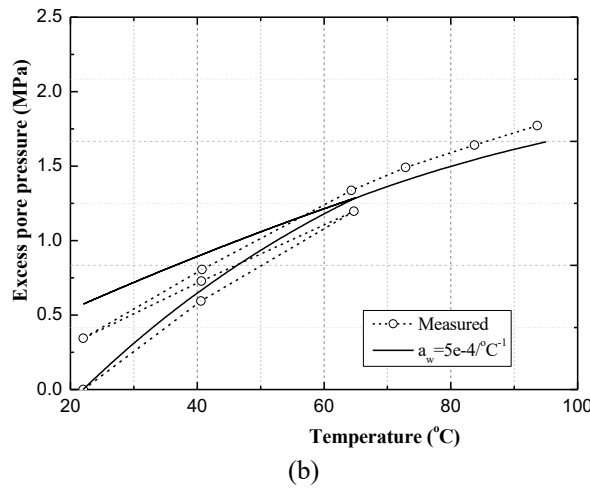
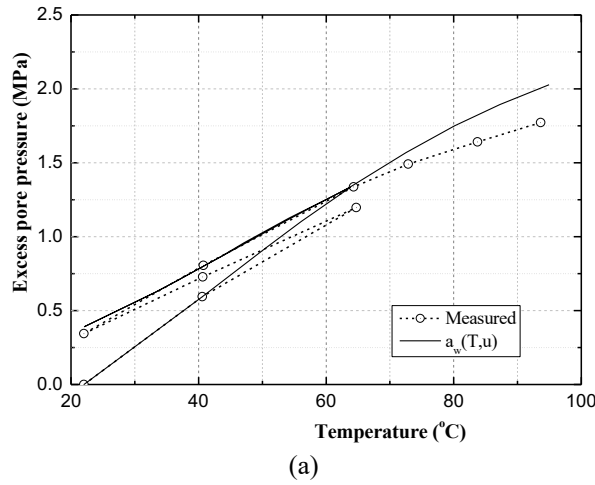


**Fig. 8** Undrained heating-cooling test on reconstituted Pontida Clay: (a)  $\alpha_w(T, u)$ ; (b) constant  $\alpha_w$

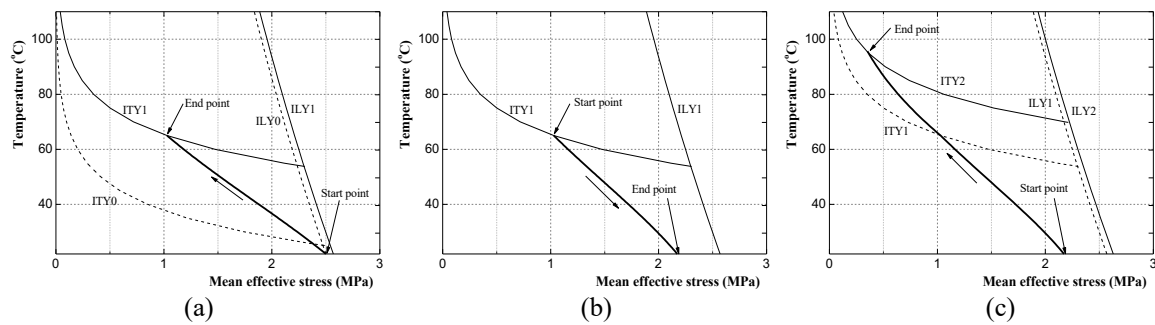


**Fig. 9** Effective stress path of undrained isotropic heating-cooling test on reconstituted Pontida Clay with  $\alpha_w(T, u)$ : (a) 22 °C to 65 °C; (b) 65 °C to 22 °C; (c) 22 °C to 95 °C

#### *6.4 Discussion of the simulation results*

The above numerical simulation results show that the undrained heating behaviors of both natural Boom Clay and reconstituted Pontida Clay are deeply affected by the volumetric thermal expansion coefficient of pore water. Different from reconstituted Pontida Clay,  $\alpha_w=5\times 10^{-4} \text{ }^\circ\text{C}^{-1}$  gives better simulation results under undrained heating test of Boom clay. One possible reason is that a large amount of adsorbed water exists in pores of this low porosity clay, and that the thermal properties of this water are affected by the physical interactions with the pore walls. Depending on its fraction with respect to the total water amount, adsorbed water can sharply change the effective thermal expansion of pore water. Determining these properties is not an easy task since they certainly depend on the clay material.

It should be emphasized that the estimation of such effective thermal properties requires macro-experimental observations combined with a back analysis and a calibration exercise. A deeper insight could be obtained from a microscale point of view. Recently, Brochard and co-workers have investigated this aspect from a fundamental point of view using molecular dynamics. Interested readers are referred to [36,37] for more details. Further systematic study on the effective thermal expansion coefficient of pore water and the corresponding mechanisms are therefore needed for better describing the undrained thermomechanical behaviour of clays.

### **7. Conclusion**

The thermo-hydro-mechanical equations proposed by Campanella and Mitchell [14], Lewis and Schrefler [17] and Coussy [18] were presented. A comparison of these three different approaches was made. The work of Campanella and Mitchell [14] has been revisited and same equations as those derived by Lewis and Schrefler [17], and Coussy [18] were obtained in the thermo-elastic state, showing their general compatibility and some differences.

A thermo-elasto-plastic model for saturated soils accounting for multiple surface plasticity and called TEAM was extended to undrained conditions in the framework of thermo-poro-mechanics. Contrary to conventional critical state models, this model is capable to predict a smooth transition between the elastic and elastoplastic states. This extension to undrained conditions required the introduction of two additional physical parameters for the water phase:

volumetric thermal expansion coefficient of pore water  $\alpha_w$ , and pore water compressibility  $C_w$ . It was demonstrated that the mineral solid compressibility  $C_s$  can be neglected in the case of clayey soils ( $C_s$  being much smaller than  $C'_d$ ).

Comparisons with experimental results on natural Boom Clay and reconstituted Pontida Clay suggest that TEAM model is able to capture the evolution of pore water pressure of saturated clays in non-isothermal undrained conditions, especially the irreversible response of pore water pressure in a heating-cooling process.

More systematic studies on the thermal expansion of pore water in low-porosity media should be conducted, including at the molecular scale, for better describing the undrained thermal behavior of clayey soils and rocks.

### **Acknowledgements**

The authors wish to acknowledge the support of the European Commission by the Marie Skłodowska-Curie Actions HERCULES - Towards Geohazards Resilient Infrastructure Under Changing Climates (H2020-MSCA-RISE-2017, 778360); Pengyun Hong wants to thank the support of National Natural Science Foundation of China (51608188).

### **Reference:**

- [1] B. Spang, Excel add-in for properties of water and steam in si-units, available from <http://www.cheresources.com/iapwsif97.shtml>, 2002 (2002).
- [2] P. Y. Hong, J. M. Pereira, A. M. Tang, Y. J. Cui, On some advanced thermo-mechanical models for saturated clays, *International Journal for Numerical and Analytical Methods in Geomechanics* 37 (17) (2013) 2952–2971.
- [3] H. Seneviratne, J. Carter, D. Airey, J. Booker, Review of models for predicting the thermomechanical behaviour of soft clays, *International Journal for Numerical and Analytical Methods in Geomechanics* 17 (10) (1993) 715–733.
- [4] M. Mohajerani, P. Delage, J. Sulem, M. Monfared, A.-M. Tang, B. Gatmiri, A laboratory investigation of thermally induced pore pressures in the callovo-oxfordian claystone, *International Journal of Rock Mechanics and Mining Sciences* 52 (2012) 112–121.

- [5] A. Gens, J. Vaunat, B. Garitte, Y. Wileveau, In situ behaviour of a stiff layered clay subject to thermal loading: observations and interpretation, *Géotechnique* 57 (2) (2007) 207–228.
- [6] T. Hueckel, M. Borsetto, Thermoplasticity of saturated soils and shales. constitutive equations, *Journal of geotechnical engineering* 116 (12) (1990) 1765 – 1777.
- [7] J.-C. Robinet, A. Rahbaoui, F. Plas, P. Lebon, Constitutive thermomechanical model for saturated clays, *Engineering Geology* 41 (1-4) (1996) 145–169.
- [8] Y. Cui, N. Sultan, P. Delage, A thermomechanical model for saturated clays, *Canadian Geotechnical Journal* 37 (3) (2000) 607–620.
- [9] H. Abuel-Naga, D. Bergado, A. Bouazza, G. Ramana, Volume change behaviour of saturated clays under drained heating conditions: Experimental results and constitutive modeling, *Canadian Geotechnical Journal* 44 (8) (2007) 94–956.
- [10] L. Laloui, François, Acmege-t: Soil thermoplasticity model, *Journal of Engineering Mechanics* 135 (2009) 932–944.
- [11] Y. Yao, A. Zhou, Non-isothermal unified hardening model: a thermo-elasto-plastic model for clays, *Géotechnique* 63 (15) (2013) 1328–1345.
- [12] T. Hueckel, R. Pellegrini, Thermoplastic modeling of undrained failure of saturated clay due to heating, *Soils and Foundations* 31 (3) (1991) 1–16.
- [13] M. Monfared, J. Sulem, P. Delage, M. Mohajerani, On the THM behaviour of a sheared boom clay sample: Application to the behaviour and sealing properties of the EDZ, *Engineering Geology* 124 (2012) 47–58.
- [14] R. Campanella, J. Mitchell, Influence of temperature variations on soil behavior, *Journal of the Soil Mechanics and Foundations Division, ASCE* 94 (1968) 709–734.
- [15] N. Khalili, A. Uchaipichat, A. Javadi, Skeletal thermal expansion coefficient and thermo-hydro-mechanical constitutive relations for saturated homogeneous porous media, *Mechanics of materials* 42 (6) (2010) 593–598.
- [16] J. Graham, N. Tanaka, T. Crilly, M. Alfaro, Modified cam-clay modelling of temperature effects in clays, *Canadian Geotechnical Journal* 38 (3) (2001) 608–621.
- [17] R. W. Lewis, B. A. Schrefler, The finite element method in the static and dynamic deformation and consolidation of porous media, John Wiley, New York, 1987.
- [18] O. Coussy, Poromechanics, John Wiley & Sons Inc, 2004.
- [19] S. Ghabezloo, J. Sulem, J. Saint-Marc, The effect of undrained heating on a fluid-saturated hardened cement paste, *Cement and Concrete Research* 39 (1) (2009) 54–64.

- [20] G. Baldi, T. Hueckel, R. Pellegrini, Thermal volume changes of the mineral-water system in low-porosity clay soils, *Canadian geotechnical Journal* 25 (4) (1988) 807–825.
- [21] P. Low, Nature and properties of water in montmorillonite-water systems, *Soil Science Society of America Journal* 43 (4) (1979) 651–658.
- [22] B. Derjaguin, V. Karasev, E. Khromova, Thermal expansion of water in fine pores, *Journal of colloid and interface science* 109 (2) (1986) 586–587.
- [23] P. Y. Hong, J. M. Pereira, Y. J. Cui, A. M. Tang, A two-surface thermo-mechanical model for saturated clays, *International Journal for Numerical and Analytical Methods in Geomechanics* 40 (7) (2016) 1059-1080.
- [24] G. Ranjan, A. Rao, Basic and applied soil mechanics, New Age International, 2007.
- [25] D. McTigue, Thermoelastic response of fluid-saturated porous rock, *Journal of Geophysical Research* 91 (B9) (1986) 9533–9542.
- [26] A. Skempton, Effective stress in soils, concrete and rocks, in: *Pore Pressure and Suction in Soils*, Butterworths, London, 1961, pp. 4–16.
- [27] G. McDowell, K. Hau, A generalised modified cam clay model for clay and sand incorporating kinematic hardening and bounding surface plasticity, *Granular Matter* 6 (1) (2004) 11–16.
- [28] J. R. Cooper, et al., Revised release on the iapws industrial formulation 1997 for the thermodynamic properties of water and steam, *The International Association for the Properties of Water and Steam* (2007) 1–48.
- [29] W. Wagner, J. Cooper, A. Dittmann, J. Kijima, H. Kretzschmar, A. Kruse, R. Mareš, K. Oguchi, H. Sato, I. Stöcker, et al., The iapws industrial formulation 1997 for the thermodynamic properties of water and steam, *Journal of Engineering for Gas Turbines and Power* 122 (2000) 150–182.
- [30] G. Baldi, T. Hueckel, A. Peano, R. Pellegrini, Developments in modelling of thermo-hydro-geomechanical behaviour of boom clay and clay-based buffer materials, Commission of the European Communities, Nuclear Science and Technology (1991) EUR 13365/1 and EUR 13365/2.
- [31] P. Delage, T. T. Le, A. M. Tang, Y. J. Cui, X. L. Li, Suction effects in deep boom clay block samples, *Géotechnique* 57 (1) (2007) 239–244.
- [32] S. Horseman, M. Winter, D. Entwistle, Geotechnical characterization of boom clay in relation to the disposal of radioactive waste, Final report, EUR 10987. Luxembourg: Commission of the European Communities.

- [33] G. Baldi, M. Borsetto, T. Hueckel, E. Tassoni, Thermally induced strains and pore pressure in clays, in: *Proceedings of the International Symposium on Environmental Geotechnology*, Allentown, Pennsylvania, 1986, pp. 391–402.
- [34] B. François, L. Laloui, C. Laurent, Thermo-hydro-mechanical simulation of ATLAS in situ large scale test in Boom Clay, *Computers and Geotechnics* 36 (4) (2009) 626-640.
- [35] G. J. Chen, X. Sillen, J. Verstricht, X. L. Li, ATLAS III in situ heating test in boom clay: Field data, observation and interpretation, *Computers and Geotechnics* 38 (5) (2011) 683-696.
- [36] L. Brochard, T. Honorio, Revisiting thermo-poro-mechanics under adsorption. Part 1: Formulation without assuming Gibbs-Duhem equation, *International Journal of Engineering Science* (under revision).
- [37] L. Brochard, T. Honorio, Revisiting thermo-poro-mechanics under adsorption. Part 2: Application to the anomalous thermal pressurization of water in undrained clays, *International Journal of Engineering Science* (under revision).
- [38] R. W. Lewis, C. E. Majorana, B. A. Schrefler, A Coupled Finite Element Model for the Consolidation of Nonisothermal Elastoplastic Porous Media, *Transport in porous media* 1(2) (1986) 155-178.
- [39] T. Hueckel, B. François, L. Laloui, Explaining thermal failure in saturated clays, *Geotechnique* 59 (3) (2009) 197-212.
- [40] P. Y. Hong, J. M. Pereira, A. M. Tang, Y. J. Cui, A two-surface plasticity model for stiff clay, *Acta Geotechnica* 11 (4) (2016) 871–885.
- [41] O. Coussy, *Mechanics and physics of porous solids*, John Wiley & Sons Inc, 2010.